RSC Advances

PAPER

View Article Online
View Journal | View Issue

Cite this: *RSC Adv.*, 2017, **7**, 50603

Formation mechanism of thermally expandable microspheres of PMMA encapsulating $NaHCO_3$ and ethanol *via* thermally induced phase separation

Shuqian Zhou, Zhengfa Zhou,* ChenRan Ji, Weibing Xu,* Haihong Ma, Fengmei Ren and Xuefan Wang

Received 12th September 2017
Accepted 17th October 2017

DOI: 10.1039/c7ra10132e

rsc.li/rsc-advances

Thermally expandable microspheres (TEMs), employing PMMA as the shell and $NaHCO_3$/ethanol as the core, were prepared *via* thermally induced phase separation (TIPS). The addition of $NaHCO_3$ improves the foaming properties of the TEMs. A mechanism for TEMs formation was proposed, comprising the following steps: (1) the separation of homogeneous polymer solutions into polymer-rich and polymer-poor phases upon cooling, where decreases in both interfacial tension and interfacial free energy (ΔG) facilitate sphere formation in a polymer-rich phase located in the polymer-poor phase; (2) the deposition of PMMA and shell formation at the interface, aided by the acute contact angle (θ) and positive spreading coefficient (S); (3) the constant deposition of PMMA shells from both the polymer-rich phase and polymer-poor phase upon cooling; and (4) the detachment of TEMs from each other facilitated by shear force from stirring. This mechanism was supported by calculations, and the effects of quench rates and stirring speeds.

1 Introduction

Thermally expandable microspheres (TEMs), commonly used as blowing agents or lightweight materials, are usually prepared *via* suspension polymerization.[1] TEMs contain core–shell structures, and thermoplastic polymers (*e.g.*, poly(acrylonitrile), poly(methyl methacrylate) and poly(vinylidene chloride)) serve as shell materials. Meanwhile, organic compounds with low boiling points, such as *i*-butane, *n*-hexane and petroleum ether, are employed as blowing agents.[2,3]

Thermally induced phase separation (TIPS) is a widely used technique that can be used to prepare scaffolds for tissue engineering purposes[4,5] and porous membranes.[6] TIPS involves cooling a homogeneous polymer solution to a temperature where the single-phase system becomes thermodynamically unstable and spontaneously separates into a polymer-rich phase and a polymer-poor phase.[7] Wu *et al.*[8] prepared PVDF/PAN blend porous membranes *via* TIPS, which can be used as separators in lithium ion batteries. Moreover, Önder and coworkers[9] have fabricated rigid poly(lactic acid) foams *via* TIPS.

The mechanism involved in TIPS technology has been investigated. Witte *et al.*[10] and Boomgaard *et al.*[11] demonstrated that a spinodal phase diagram could explain the mechanism. They concluded that liquid–liquid separation begins in the demixing gap to form porous structures. Meanwhile, the liquid–liquid demixing gap is subdivided into a region of spinodal demixing that is bounded by the spinodal. Then two regions of nucleation and growth between the binodal and the spinodal are formed. Nishi *et al.*[12] studied the TIPS mechanism for polystyrene-poly(vinyl-methyl ether) mixtures using light transmission, optical microscope and pulsed NMR studies. These efforts revealed that phase separation occurred either *via* a spinodal mechanism or *via* a nucleation and growth mechanism. Tompa[13] and Altena *et al.*[14] calculated phase diagrams for ternary systems of amorphous polymers using binary interaction parameters, where the results supported a nucleation and growth mechanism. Mannella *et al.*[15] investigated the TIPS behavior of a poly(L-lactide)-dioxane–water system directly by means of cloud point detection *via* light transmittance measurements, and indirectly through the preparation of several porous foams. Considerable pore dimension variation was noted with variations in holding time, holding temperature and poly(L-lactide) concentration; the results also supported a nucleation and growth mechanism.

Ogawa *et al.*[16] prepared poly(methyl methacrylate) foamable particles *via* TIPS from a PMMA/ethanol mixture. Unfortunately, the foamable particles possessed poor foaming properties, being only twice the size of the original particles even under vacuum foaming conditions.

In this work, TEMs with PMMA as the shell and $NaHCO_3$/ethanol solution as the core were prepared *via* the simple method of TIPS. The addition of $NaHCO_3$ improved the TEMs foaming properties. The mechanism for TIPS-based TEMs formation was probed *via* the following methods: (1) measuring the contact angle (θ) and tension (γ_{gl}) at different temperatures; (2)

School of Chemistry and Chemical Engineering, Hefei University of Technology, Hefei, 230009, The People's Republic of China. E-mail: weibingxu@hfut.edu.cn; zhengfazhou@hfut.edu.cn; Tel: +86-0551-62901455

calculating the interfacial free energy (ΔG) and spreading coefficient (S) with changing temperature; and (3) investigating the effects of quenching rate and stirring speed on the morphologies of the TEMs. To the best of our knowledge, there are few reports investigating the formation mechanism of TEMs *via* TIPS.

2 Experimental

2.1 Materials

Reagent grade $NaHCO_3$, ethanol, and PMMA ($M_w = 5.05 \times 10^4$, $M_w/M_n = 1.15$) were all obtained from Sinopharm, China. All chemicals were used as received without further purification.

2.2 Thermally induced phase separation experiments

50 g of ethanol, 3 g of $NaHCO_3$ and 0.5 g of PMMA were added to a 100 mL glass vessel, which was equipped with an agitator, a condenser (Allihn type), and a thermometer. A schematic diagram of the apparatus is shown in Fig. 1. The entire apparatus was submerged in a 60 °C water bath. The mixture was stirred at 100 rpm for 1 h, and a homogeneous solution was obtained. Then the apparatus was quickly transferred to an ice-water bath, where it was cooled to 5 °C with different quenching times or stirring speeds. The quenching time was set at 2 min, 10 min, 30 min, or 60 min with a stirring speed of 200 rpm; or the stirring speed was set at 0 rpm, 100 rpm, 200 rpm, 300 rpm, 400 rpm, or 500 rpm with a quenching time of 2 min. The mixture had a slightly opaque color. The mixture was filtered under vacuum filtration with a membrane filter size of 0.1 μm. TEMs were obtained after washing successively with distilled water and ethanol, and drying in an oven at 30 °C for 2 h.

2.3 Characterization

Scanning electron microscope (SEM) images of the TEMs were collected on a scanning electron microscope (SU8020, Shimadzu, Japan); samples for SEM imaging were deposited on Cu wafers. Each sample was sputter-coated with a thin layer of gold to prevent sample-charging problems.

The contact angle (θ) was determined using contact angle measurements (DSA100, Kruss, Germany). Ethanol/$NaHCO_3$ solution and PMMA were put into beakers with closed lids. The temperature was set at 5 °C, 10 °C, 19 °C, 31 °C, 40 °C, 49 °C, or 58 °C.

The surface tension was analyzed using a surface tensiometer (BYZ-1, Hengping, China). The samples of ethanol/$NaHCO_3$ solution were the same as those used for contact angle measurements.

The particle size distribution was measured using a laser scattering particle size analyzer (LS, MS-2000, Malvern). TEMs were dispersed in deionized water under ultrasonic dispersion for 5 min.

The encapsulated ethanol and $NaHCO_3$ content were investigated using a thermal gravimetric analyser (TGA, NETZSCH, 209F3). The samples were heated from 30 °C to 900 °C at a rate of 2 °C min^{-1} under a nitrogen atmosphere.

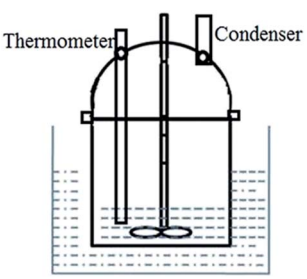

Fig. 1 A schematic diagram of the apparatus.

3 Results and discussion

3.1 Formation mechanism of TEMs *via* TIPS

0.5 g of PMMA and 3 g of $NaHCO_3$ were dissolved in 50 g of ethanol at 60 °C, and a uniform phase solution was obtained (Fig. 2(a)). The uniform phase separated into a polymer-poor phase and a polymer-rich phase when the temperature was reduced,[9] and an interface formed between the polymer-poor phase (outer) and the polymer-rich phase (inner). In the PMMA/$NaHCO_3$/ethanol mixture a demixing polymer mechanism supported a spinodal one, which contains a polymer-rich phase, a polymer-poor phase and the interface. Meanwhile, the PMMA chains might transform from a random style to an oriented style under the shear force from stirring (Fig. 2(b) and (c)).

Next, PMMA deposition is initiated firstly in the polymer-rich phase where PMMA forms a shell at the interface between the polymer-poor phase and polymer-rich phase. The evidence for the aforementioned mechanism is as follows. (1) The interfacial tension generated between the polymer-poor phase and polymer-rich phase causes the polymer-rich phase to form droplets.[17] In addition, the interfacial free energy decreases with cooling, and the decrease in interfacial free energy also facilitates the polymer-rich phase forming spheres within the polymer-poor phase. (2) Vold[17] found that a liquid could form a concave interface and a solid could be spontaneously wetted on the liquid surface when the contact angle was less than 90°. Since the contact angle of the ethanol/$NaHCO_3$ solution on the PMMA surface was less than 90°, the ethanol/$NaHCO_3$ solution could form a concave interface and PMMA had the tendency to deposit on the ethanol/$NaHCO_3$ solution surface. (3) Good and Fowkes[17] proposed that a spreading coefficient greater than zero facilitates a shell material encapsulating a core material. The experimental results indicated the spreading coefficient between the polymer-rich phase and the polymer-poor phase was positive. The ethanol/$NaHCO_3$ solution could thus be encapsulated by PMMA. (4) Mannella *et al.*[15] prepared a poly-L-lactide porous membrane *via* TIPS. In this work, it was postulated that the microspheres might have physical contact with each other. The formation of TEMs was deemed unfeasible without stirring. The effect of shear forces from stirring might orient the PMMA chains and facilitate the formation of TEMs,[18,19] and also keep microspheres separate from each other. Therefore, PMMA formed the shells and ethanol/$NaHCO_3$ solution formed the core materials upon cooling and stirring (Fig. 2(d)).

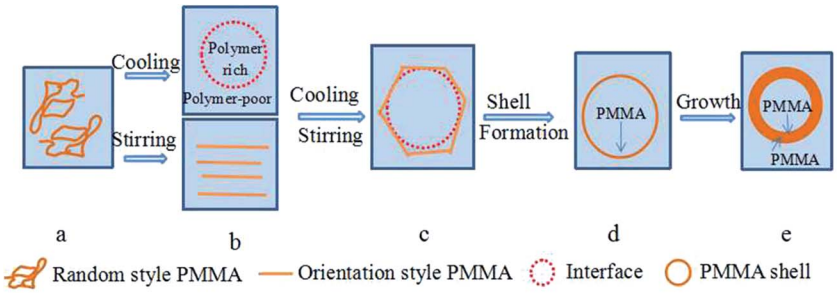

Fig. 2 A schematic diagram of the mechanism for the formation of microspheres with a core–shell structure *via* TIPS, depicting (a) a uniform phase solution; (b) the existence of polymer-rich and polymer-poor phases, and oriented PMMA molecules; (c and d) PMMA shell formation; and (e) PMMA shell growth.

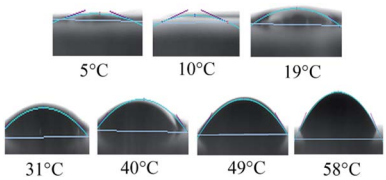

Fig. 3 Shapes of the contact angles between ethanol/$NaHCO_3$ solution and a PMMA surface under a balanced state at different temperatures.

Thereafter, the shell grew as PMMA was deposited constantly from the polymer-rich phase and polymer-poor phase due to further decreases in temperature, and disjointed microspheres were obtained upon stirring (Fig. 2(e)). As a result, TEMs were obtained. A schematic representation of the mechanism is shown in Fig. 2.

3.2 Shell-formation

The interfacial free energy between the PMMA and $NaHCO_3$/ethanol solutions is related to the temperature according to the Gibbs free energy.[20] Harkins defined the spreading coefficient as the reduction in interfacial free energy per unit area.[17] Vold proposed that interfacial free energy, interfacial tension, and the spreading coefficient could be described as shown in eqn (1).[17]

$$\Delta G = -S = \gamma_{gs} - \gamma_{gl} - \gamma_{ls} \quad (1)$$

where ΔG is the difference in interfacial free energy, S is the spreading coefficient, and γ_{gs}, γ_{gl}, and γ_{ls} are the interfacial tension values between gas and solid, gas and liquid, and liquid and solid, respectively.

According to the Young equation, the relation between γ_{gs}, γ_{ls} and γ_{gl} can be described as shown in eqn (2).[21]

$$\gamma_{gs} = \gamma_{ls} + \gamma_{gl} \cos\theta \quad (2)$$

where θ is the contact angle between the ethanol/$NaHCO_3$ solution and the PMMA surface in a balanced state.

Eqn (3) can be obtained through combining eqn (1) and (2).

$$\Delta G = -S = -\gamma_{gl}(\cos\theta - 1) \quad (3)$$

where θ was analyzed through contact angle measurements, and was determined at 5 °C, 10 °C, 19 °C, 31 °C, 40 °C, 49 °C, and 58 °C. The shapes of the contact angles between the ethanol/$NaHCO_3$ solution and PMMA surface under a balanced state at different temperatures are shown in Fig. 3; the values of θ are shown in Table 1. θ was less than 90 degrees during the process of TIPS, and θ increased with decreasing temperature. According to Vold's theory,[17] since the contact angle between the ethanol/$NaHCO_3$ solution and PMMA surface was less than 90°, the ethanol/$NaHCO_3$ solution could form a concave interface. PMMA had the tendency to be wetted on the ethanol/$NaHCO_3$ solution surface; this provided the conditions for PMMA to deposit at the interface between the polymer-rich phase and polymer-poor phase.

The tension between gas and liquid (γ_{gl}) was determined using a surface tensiometer. Values of γ_{gl} were determined at 5 °C, 10 °C, 19 °C, 31 °C, 40 °C, 49 °C, and 58 °C. The results indicated that γ_{gl} increased with decreasing temperature (Table 1).

Table 1 γ_{gl}, θ, S and ΔG data at different temperatures

Temperature (°C)	θ (°)					γ_{gl} (mN m^{-1})						
	1	2	3	Average	SD	1	2	3	Average	SD	ΔG (J mol^{-1})	S
5	5.58	5.63	5.62	5.61	0.022	23.7	23.8	23.8	23.8	0.057	−0.12	0.12
10	6.31	6.33	6.29	6.31	0.017	23.4	23.7	23.6	23.6	0.22	−0.15	0.15
19	8.18	8.23	8.22	8.21	0.037	23.5	23.7	23.1	23.4	0.25	−0.3	0.3
31	9.25	9.25	9.22	9.24	0.012	22.5	22.8	22.8	22.7	0.14	−0.41	0.41
40	10.91	10.93	10.94	10.93	0.013	22.2	22.4	22.4	22.4	0.12	−0.42	0.42
49	17.25	17.29	17.27	17.27	0.016	21.8	21.9	21.5	21.7	0.17	−0.98	0.98
58	25.14	25.13	25.09	25.12	0.022	21.4	21.6	21.6	21.5	0.10	−2.04	2.04

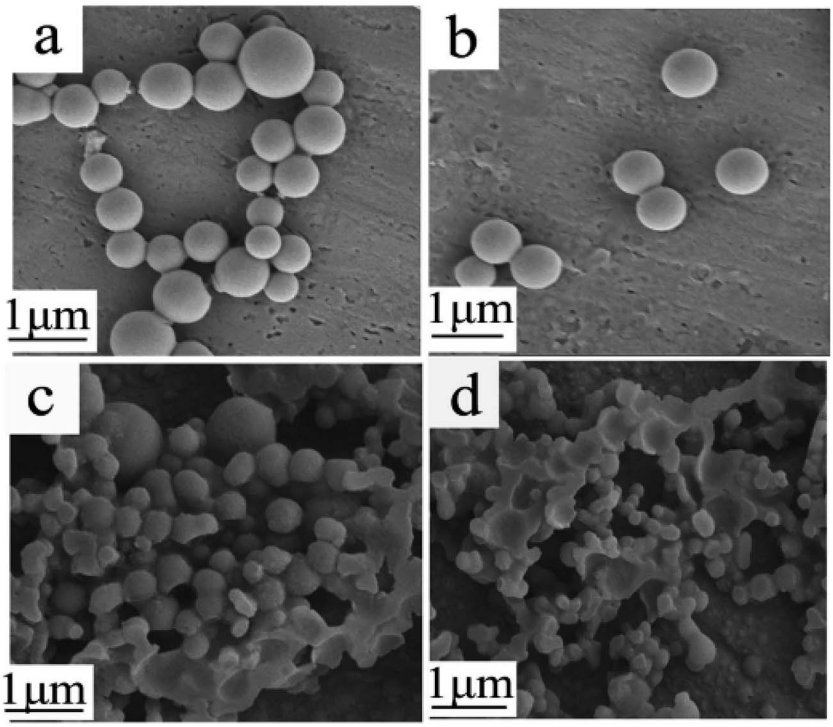

Fig. 4 SEM images of TEMs prepared with different quench times: (a) 2 min; (b) 10 min; (c) 30 min; and (d) 60 min.

The values of ΔG and S were obtained using eqn (3) (Table 1). The interfacial free energy decreased when the temperature was reduced from 58 °C to 5 °C, providing the conditions for the polymer-rich phase to form spheres among the polymer-poor phase. S decreased with decreasing temperature and remained positive during the process of TIPS. Based on the theory of Good and Fowkes,[17] there existed a tendency for the ethanol/$NaHCO_3$ solution to be encapsulated by PMMA when the spreading coefficient was positive.

On the basis of the calculation results, we concluded that PMMA could form a shell at the interface between the polymer-rich phase and polymer-poor phase while ethanol/$NaHCO_3$ solution could be encapsulated by PMMA. Microspheres with a core–shell structure were formed.

3.3 Effects of quench rate and quench time

The mixture of ethanol/$NaHCO_3$ and PMMA was quenched from 60 °C to 5 °C within 2 min, 10 min, 30 min or 60 min, under a stirring speed of 200 rpm. The TEMs obtained were characterized using SEM (images shown in Fig. 4). The TEMs were fully spherical when the quenching time was 2 min (Fig. 4(a)) or 10 min (Fig. 4(b)). However, when the quenching time was greater than 30 min, some PMMA formed complete spheres while some formed hemispheres (Fig. 4(c)). The proportion of hemispheres increased with an increase in quench times (Fig. 4(d)). Meanwhile, the percentages and diameters of the microspheres were influenced by the quench rate. A reasonable explanation was that a high quenching rate led to a lower amount of PMMA diffusing from the polymer-rich phase to the polymer-poor phase. Consequently, PMMA could quickly deposit at the interface between the polymer-rich phase and the polymer-poor phase. However, a slow quenching rate allowed enough time for PMMA to diffuse from the polymer-rich phase to the polymer-poor phase; the small concentration difference led to much worse interfacial stability. Therefore, the core–shell structure of some spheres was incomplete. The experimental results also provided evidence for the suggested mechanism.

Samples were extracted from the experimental apparatus at 60 °C, 28 °C, 10 °C and 5 °C during the quenching of the mixture of ethanol/$NaHCO_3$ and PMMA from 60 °C to 5 °C under a stirring speed of 200 rpm. We found that the mixture began to muddy at about 28 °C in many experiments, therefore 28 °C was the cloud point of the mixture of ethanol/$NaHCO_3$ and PMMA, and 28 °C was selected as one of the temperature points. The samples were put into glass bottles which had been previously set to 60 °C, 28 °C, 10 °C or 5 °C, depending on the respective sample. A photo of the bottle was taken within 10 s, and the

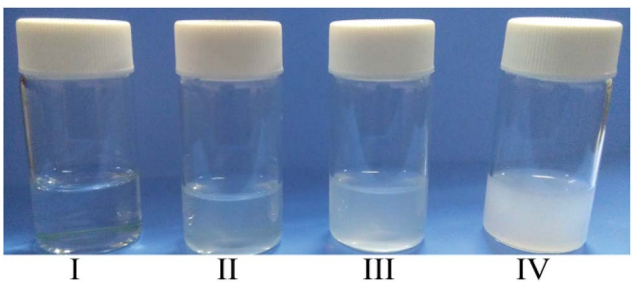

Fig. 5 Photos of mixtures of ethanol/$NaHCO_3$ and PMMA at different temperature points during quenching: (I) 60 °C; (II) 28 °C; (III) 10 °C; and IV: 5 °C.

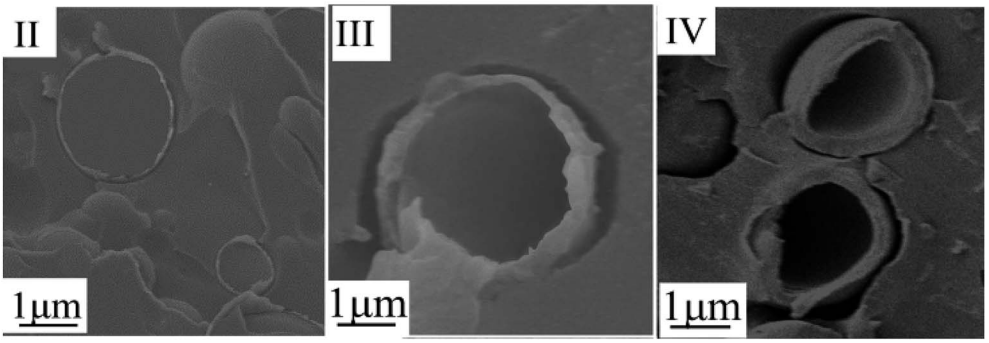

Fig. 6 SEM images of TEMs at different temperature point during quenching: (II) 28 °C; (III) 10 °C; and (IV): 5 °C.

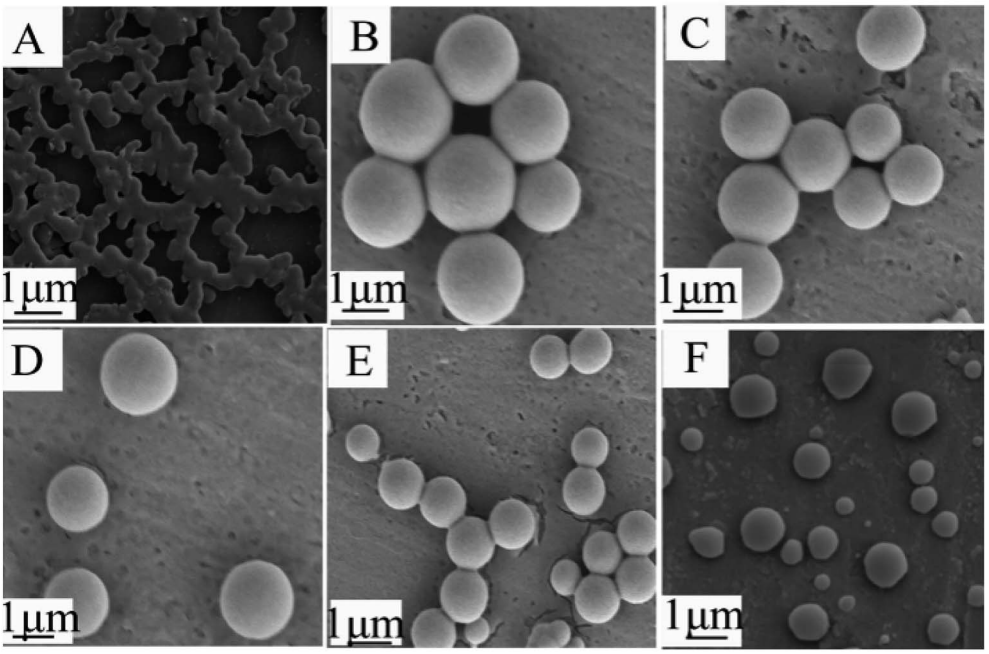

Fig. 7 SEM images of TEMs prepared at different stirring speeds: (A) 0 rpm; (B) 100 rpm; (C) 200 rpm; (D) 300 rpm; (E) 400 rpm; and (F) 500 rpm.

results are shown in Fig. 5. The mixture was transparent when the temperature was above 28 °C (Fig. 5(I)), and became muddy immediately at about 28 °C (Fig. 5(II)). The mixture turbidity increased as the temperature decreased (Fig. 5(III) and (IV)), which might be due to an increase in the amount and diameter of the TEMs.

Other samples were also extracted from the experimental apparatus at 60 °C, 28 °C, 10 °C and 5 °C, respectively, and filtrated within 10 s. No filtrate was obtained at 60 °C. The filtrate of each sample was dried in a drying oven at 30 °C, and then it was fixed with epoxy resin and cut into slices with a wallpaper knife to observe the thickness of the PMMA shell *via* SEM. The results are shown in Fig. 6. The thickness of the PMMA shell gradually increases as the temperature decreases during quenching.

3.4 Effects of stirring

The polymer chains could straighten and orientate into molecular bundles.[18] Diat *et al.*[19] investigated the effects of shear force on the orientation of lyotropic lamellar polymer molecules. They found that the kinetic instability of the fluid under the shear forces of stirring led the polymer to transform into multilayer vesicles; a single vesicle was eventually formed with increasing shear force and time. As a result, the shear force facilitated core–shell structure formation. The effects of stirring observed in our work might be the same as for lyotropic lamellar polymers. The shear force oriented the PMMA chains and facilitated TEMs formation; it also prevented microspheres from contacting each other.

The morphologies of TEMs quenched from 60 °C to 5 °C within 2 min at different stirring speeds are shown in Fig. 7. In this work, the ethanol/$NaHCO_3$ and PMMA mixture also formed a porous membrane without stirring (Fig. 7(A)). When the stirring speed was below 400 rpm, the ethanol/$NaHCO_3$ and PMMA mixture formed TEMs. The average diameter of the TEMs decreased upon increasing the stirring speed (Fig. 7(B)–(E)). TEMs were not fully spherical when the stirring speed was

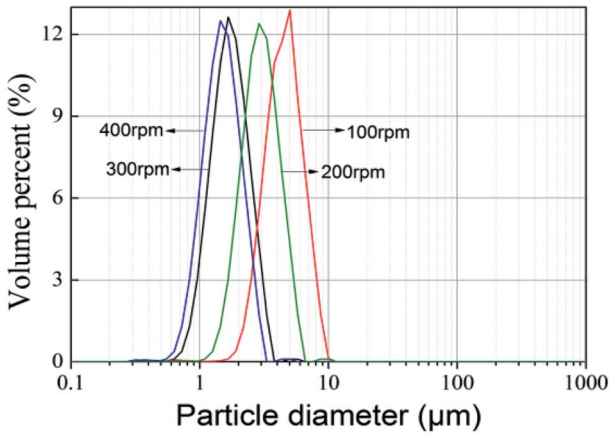

Fig. 8 Particle size distribution of TEMs prepared at different stirring speeds. Quench rate: quenching from 60 °C to 5 °C within 2 min; stirring speed: 100 rpm, 200 rpm, 300 rpm, or 400 rpm.

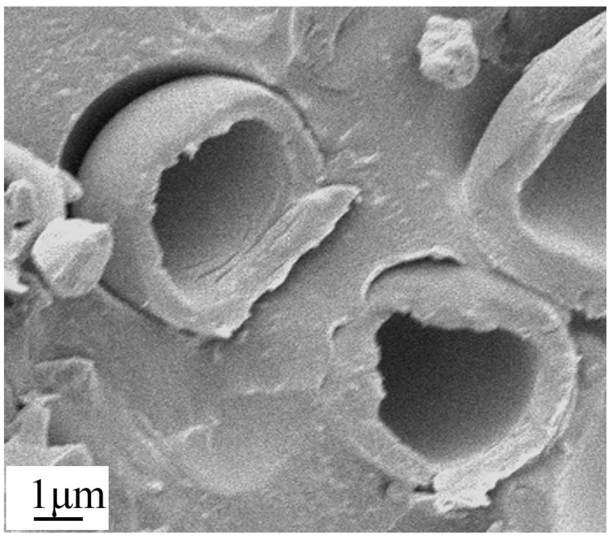

Fig. 9 SEM image of a cross section of TEMs prepared at 200 rpm upon quenching from 60 °C to 5 °C within 2 min.

500 rpm (Fig. 7(F)), and too large a shear force from stirring affected the integrity of the TEMs. Based on these results, it could be concluded that the effects of stirring might orient the PMMA chains and facilitate TEMs formation, and make TEMs disconnect from each other.

The size distribution of TEMs prepared at different stirring speeds is shown in Fig. 8. The average diameters of TEMs with stirring speeds of 100 rpm, 200 rpm, 300 rpm, and 400 rpm are 4.3 μm, 3.1 μm, 2.5 μm and 2.1 μm, respectively. Jonsson[22] and Kim *et al.*[3] found that the diameter of TEMs prepared *via* suspension polymerization decreased upon increasing the stirring speed. In this work, the diameters of TEMs from TIPS were also found to inversely correlate with stirring speed. Namely, TEMs with different diameters could be obtained by controlling the stirring speed; this means the cell size of foaming materials could be easily adjusted for various applications.

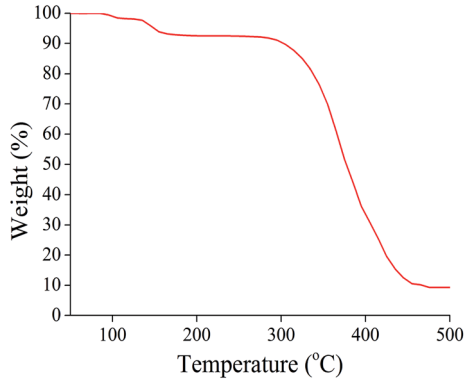

Fig. 10 TG analysis of TEMs prepared at 200 rpm upon quenching from 60 °C to 5 °C within 2 min.

3.5 Core-shell structure and foaming properties

The core–shell structure and foaming properties of typical TEMs, which were prepared by quenching from 60 °C to 5 °C within 2 min under stirring at 200 rpm, were investigated. To verify the core–shell structure of the TEMs, the TEMs were fixed with epoxy resin and cut into slices. Fig. 9 shows an image of the cross section of the TEMs; it clearly shows that TEMs present a hollow inner and outer shell structure.

The ethanol and $NaHCO_3$ content was analyzed *via* TG analysis (Fig. 10). The weight loss of ethanol over the range from 102 °C to 115 °C in the first step was about 2.2%. The weight loss of CO_2 upon $NaHCO_3$ decomposition over the range from 115 °C to 165 °C in the second step was 5.1%. The PMMA shell decomposed at about 320 °C. The residue coming from $NaHCO_3$

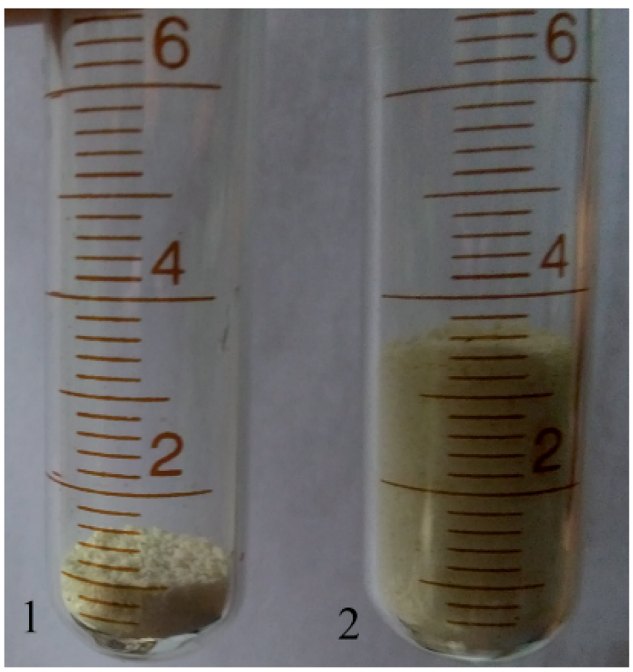

Fig. 11 Digital photographs of unexpanded (1) and expanded (2) TEMs at 120 °C.

was about 6.3%. Therefore the calculated encapsulated ethanol and $NaHCO_3$ content was 2.2% and 11.4%, respectively.

The TEMs were heated to 120 °C in an oven for 30 min to investigate the foaming properties. Digital photographs of unexpanded and expanded TEMs are shown in Fig. 11. The TEMs were calibrated at 1 cm before foaming (Fig. 11(1)). The maximum expansion volume of the TEMs was about 3.5 times the original volume under ambient pressure (Fig. 11(2)).

4 Conclusions

A PMMA and ethanol/$NaHCO_3$ homogeneous solution separated into a polymer-rich phase and a polymer-poor phase upon decreasing the temperature, and an interface formed. First, the interfacial tension and a reduction in interfacial free energy led the polymer-rich phase to form spheres among the polymer-poor phase. Second, since the contact angle between the ethanol/$NaHCO_3$ solution and the PMMA surface was less than 90°, the ethanol/$NaHCO_3$ solution could form a concave interface where PMMA could deposit. Third, as the spreading coefficient between the polymer-rich phase and polymer-poor phase was positive, PMMA could encapsulate the ethanol/$NaHCO_3$ solution. Finally, the shear force from stirring facilitated TEMs formation while separating TEMs from each other. Therefore, PMMA could form a shell, and the shell grew as the temperature decreased further due to a decrease in the solubility of PMMA. A higher quench rate suppressed the diffusion of PMMA from the polymer-rich to the polymer-poor layer. As a result, PMMA could quickly deposit and fix at the interface. TEMs with different diameters could be obtained by controlling the stirring speed. Based on the calculation results, and the effects of quench rate and stirring speeds on the morphologies of the TEMs, the proposed formation mechanism for TEMs *via* TIPS was reasonable.

Conflicts of interest

There are no conflicts to declare.

Acknowledgements

The authors are grateful for financial support from the Fundamental Research Funds for the Central Universities (JD2016JGPY002 and JZ2017YYPY0241).

References

1 J. R. Mi, H. Jung, J. U. Ha, S. H. Baeck and E. S. Sang, *Colloid Polym. Sci.*, 2017, **29**, 171–180.
2 M. Safajou-Jahankhanemlou, F. Abbasi and M. Salami-Kalajahi, *Colloid Polym. Sci.*, 2016, **294**, 1–10.
3 J. G. Kim, U. H. Jin, K. J. Sun, K. Lee and S. H. Baeck, *Colloid Polym. Sci.*, 2015, **293**, 3595–3602.
4 F. A. Jahwari, A. A. W. Anwer and H. E. Naguib, *J. Polym. Sci., Part B: Polym. Phys.*, 2015, **53**, 795–803.
5 Z. Q. Guo, C. Yang, Z. P. Zhou, S. Chen and F. Li, *RSC Adv.*, 2017, **54**, 34063–34070.
6 C. Zeiger, J. Kumberg, F. Vullers, M. Worgull, H. Holscher and M. N. Kavalenka, *RSC Adv.*, 2017, **52**, 32806–32811.
7 J. T. Fu and J. M. Torkelson, *Macromolecules*, 1990, **23**, 4983–4989.
8 Q. Y. Wu, H. Q. Liang, L. Gu, Y. Yu, Y. Q. Huang and Z. K. Xu, *Polymer*, 2016, **107**, 54–60.
9 Ö. C. Önder, E. Yilgör and I. Yilgör, *Polymer*, 2016, **107**, 240–248.
10 P. V. D. Witte, P. J. Dijkstra, J. W. A. V. D. Berg and J. Feijen, *J. Membr. Sci.*, 2017, **117**, 1–31.
11 (*a*) T. V. D. Boomgaard, R. M. Boom and C. A. Smolders, *Macromol. Symp.*, 1990, **39**, 271–281; (*b*) R. M. Boom, H. W. Reinders, H. H. W. Rolevink, T. V. D. Boomgaard and C. A. Smolders, *Macromolecules*, 1994, **27**, 2041–2044.
12 T. Nishi, T. T. Wang and T. K. Kwei, *Macromolecules*, 1975, **8**, 17–21.
13 H. Tompa, *Polymer solutions*, Butterworths, London, 1956, p. 82.
14 F. W. Altena and C. A. Smolders, *Macromolecules*, 1982, **15**, 1491–1497.
15 G. A. Mannella, F. C. Pavia, G. Conoscenti, V. L. Carrubba and V. Brucato, *J. Polym. Sci., Part B: Polym. Phys.*, 2014, **52**, 979–983.
16 H. Ogawa, A. Ito, K. Taki and M. Ohshima, *J. Appl. Polym. Sci.*, 2010, **106**, 2825–2830.
17 R. D. Vold and M. J. Vold, *Colloid and interface chemistry*, Addison-Wesley, 1983.
18 G. Strobl, *The physics of polymers*, Springer Verlag, Berlin, 2012.
19 O. Diat and D. Roux, *J. Phys. II*, 1993, **3**, 9–14.
20 G. Strobl, *The physics of polymers*, Springer Verlag, Berlin, 2012.
21 E. Charles and J. Carraher, *Polymer Chemistry*, Florida, CRC press, 8th edn, 2010.
22 M. Jonsson, O. Nordin, E. Malmström and C. Hammer, *Polymer*, 2006, **47**, 3315–3324.